DESIGN STUDIES OF A HIGH-POWER INFRARED-TERAHERTZ FEL FACILITY

Y. M. Yang, Z. Y. Zhao, C. Chen, M. Q. Xia, Z. X. Cao, G. Y. Feng*
University of Science and Technology of China, Hefei, China

Abstract

Design studies of a high-power infrared-terahertz free-electron laser facility are presented. The facility is based on a high-repetition-rate superconducting linac and is designed to generate electron beams with energies up to about 60 MeV. A third-harmonic linearizing cavity and a C-type magnetic chicane are used to control the longitudinal phase space of the bunch. Start-to-end beam dynamics simulations show that the peak current can be increased from about 26 A to about 100 A, while keeping the normalized projected emittance below 1.2 mm mrad. Based on the optimized beam parameters, FEL oscillator simulations are performed for the mid-infrared, far-infrared and THz beamlines. The results show that cavity detuning has a significant influence on the mid-infrared output spectrum, and an appropriate detuning length helps suppress sidebands and multi-peak structures, leading to improved spectral monochromaticity. In the far-infrared range, the phase difference between transverse modes in the rectangular waveguide reduces the on-axis field intensity and leads to a clear reduction of the coupled output power around 85 µm–95 µm. In the THz range, the output power decreases more smoothly with increasing wavelength, and no pronounced narrow spectral gap is observed. These studies provide a basis for beam-parameter selection, cavity-detuning optimization and waveguide-coupling design for high-power long-wavelength FEL operation.

INTRODUCTION

Infrared and terahertz free-electron lasers (FELs) provide continuously tunable coherent radiation with high peak power and flexible pulse structures [1, 2]. They are useful for spectroscopy, materials science, molecular dynamics and nonlinear light-matter interaction [2, 3]. For these applications, high average power and high repetition rate are important for improving photon flux, data-acquisition efficiency and long-term operation stability [4, 5].

A high-power infrared-terahertz (IR-THz) FEL facility based on a high-repetition-rate superconducting linac is under study. The facility is designed to cover wavelengths from 5 µm to 1000 µm with three oscillator beamlines. The electron beam is generated from an RF gun, accelerated by superconducting cavities, linearized by a third-harmonic RF system and compressed by a magnetic chicane before being transported to the FEL oscillators.

Previous studies mainly focused on the longitudinal beam dynamics and RF-parameter optimization of the linac [6, 7]. A third-harmonic cavity was used to compensate the nonlinear curvature of the longitudinal phase space, and a C-type chicane was adopted to increase the peak current to the hundred-ampere level. Based on these beam dynamics studies, it is necessary to evaluate whether the optimized beam can support stable oscillator operation over the designed wavelength range.

In this paper, the overall layout and start-to-end beam dynamics of the proposed IR-THz FEL facility are presented. The electron bunch is compressed to a peak current of about 100 A and accelerated to about 60 MeV. Oscillator simulations are then performed for the mid-infrared, far-infrared and THz beamlines. The influence of cavity detuning on the mid-infrared output spectrum is investigated, and waveguide-related output characteristics in the far-infrared and THz ranges are discussed. These studies provide a basis for selecting the oscillator working points and for understanding the detuning and waveguide effects in a high-power long-wavelength FEL facility.

FACILITY LAYOUT AND BEAM PARAMETERS

The schematic layout of the proposed IR-THz FEL facility is shown in Fig. 1. The facility is based on a high-repetition-rate superconducting linac and is designed to drive three oscillator beamlines covering the mid-infrared, far-infrared and THz wavelength ranges. The electron beam is generated from an RF gun and accelerated to about 5 MeV. Solenoids are used in the low-energy section for transverse focusing and emittance compensation. After the gun, the beam is accelerated by a 1.3 GHz superconducting accelerating section. A 3.9 GHz third-harmonic RF system is installed downstream of this section to linearize the longitudinal phase space before bunch compression. The beam energy before the chicane is about 20 MeV.

A C-type magnetic chicane is adopted to compress the bunch and increase the peak current to the hundred-ampere level. After compression, the beam is further accelerated by two 1.3 GHz superconducting cavities to a final energy of about 60 MeV, and then transported to different FEL oscillator beamlines by a beam distribution system. The three beamlines are designed to cover 5 µm–40 µm, 40 µm–200 µm and 200 µm–1000 µm, respectively. This layout provides a common linac platform for a wide wavelength range from the mid-infrared to the THz region.

The RF parameters of the accelerating sections were first determined using a longitudinal beam dynamics optimization method based on the higher-order transfer map of the bunch compressor [8–11]. For a fixed chicane, the longitu-

* fenggy@ustc.edu.cn

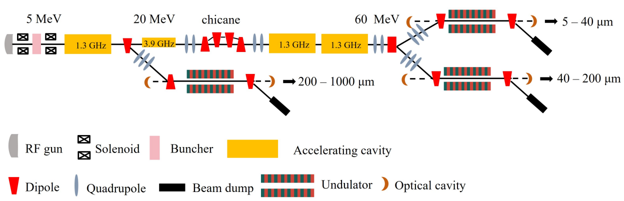

Figure 1: Schematic layout of the proposed IR-THz FEL facility.

dinal coordinate after the ith bunch compressor is written as

$$s_i = s_{i-1} - \left(R_{56i}\delta_i + T_{566i}\delta_i^2 + U_{5666i}\delta_i^3\right), \qquad (1)$$

where δ_i is the relative energy deviation, and R_{56i}, T_{566i} and U_{5666i} are the longitudinal momentum compaction terms. The RF amplitudes and phases of the fundamental and third-harmonic cavities were then adjusted to obtain the required beam energy, compression factor and longitudinal phase-space curvature. In this way, the RF settings provide an initial linear energy chirp for compression while suppressing the nonlinear distortion from the fundamental RF curvature. These parameters were subsequently used as the starting point for start-to-end beam dynamics simulations.

Figure 2 shows the simulated beam distributions at representative locations along the linac. After the RF gun, the bunch has a peak current of about 26 A, and the normalized projected emittances in both transverse directions are about 1.3 mm mrad. At this stage, the longitudinal phase space still contains a strong nonlinear curvature and is not suitable for direct magnetic compression. After acceleration and third-harmonic linearization, the peak current remains close to 26 A, while the longitudinal phase space becomes nearly linear. The normalized projected emittances are reduced to about 0.97 mm mrad in both transverse planes.

After passing through the chicane, the bunch length is significantly shortened and the peak current increases to about 100 A. Due to the bending section and collective effects, the transverse emittances increase slightly to about 1.15 mm mrad and 1.05 mm mrad in the horizontal and vertical directions, respectively. At the exit of the main linac, the beam energy reaches about 60 MeV, and the peak current is maintained at about 103 A. The final normalized projected emittances are about 1.18 mm mrad and 1.21 mm mrad. These results indicate that the optimized linac and compression scheme can provide an electron beam with sufficient peak current and acceptable transverse beam quality for the following FEL oscillator studies.

OSCILLATOR SIMULATION STUDIES

Based on the optimized electron beam parameters, FEL oscillator simulations were performed for the mid-infrared, far-infrared and THz beamlines. For an FEL oscillator, the cavity detuning determines the temporal overlap between the returned optical pulse and the electron bunch. Therefore, it has a direct influence on the output spectrum and spectral monochromaticity. Figure 3 shows the saturated spectra of

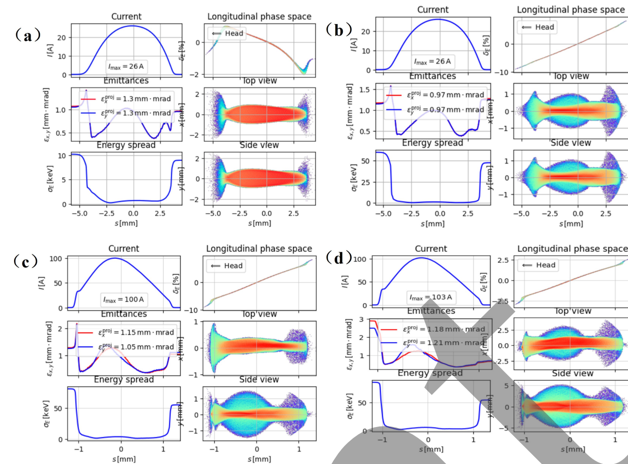

Figure 2: Start-to-end beam dynamics simulation results at representative locations: (a) after the RF gun, (b) after acceleration and third-harmonic linearization, (c) after the bunch compressor, and (d) after the main linac.

the mid-infrared FEL oscillator under different cavity detuning lengths. Two representative wavelengths, around 25 μm and 40 μm, were selected for the detuning scan. For the 25 μm case, a relatively narrow spectrum is obtained around $\Delta L = 75$ μm, while sidebands and multi-peak structures appear when the detuning length deviates from this condition. For the 40 μm case, the spectrum becomes narrower around $\Delta L = 200$ μm, whereas a reduced detuning length leads to spectral broadening and pronounced sidebands on the long-wavelength side. These results indicate that an appropriate cavity detuning length is required to suppress sidebands and improve the spectral monochromaticity of the mid-infrared oscillator.

For the far-infrared and THz beamlines, the optical mode size becomes large and the diffraction loss becomes significant. A rectangular waveguide is therefore introduced to confine the optical field in the long-wavelength range. However, the waveguide also modifies the transverse mode structure in the resonator. The phase difference between transverse modes can reduce the on-axis field intensity and affect the coupling efficiency through the output hole.

Figure 4 shows the calculated coupled output power in the far-infrared range. A clear local reduction of the output power appears around 85 μm–95 μm. This behavior is consistent with the expected spectral gap caused by transverse-mode interference in the rectangular waveguide. The transverse intensity distributions in Fig. 5 further support this interpretation. At wavelengths where the field remains concentrated near the axis, the center-hole coupling is more efficient. In contrast, when a hollow or multi-lobed distribution is formed, the on-axis intensity is reduced, leading to a decrease in the coupled output power.

The same output-power scan was performed for the THz beamline, as shown in Fig. 6. Compared with the far-infrared case, the THz output power decreases more smoothly with increasing wavelength, and no pronounced narrow spectral gap is observed. This suggests that, in the THz range, the

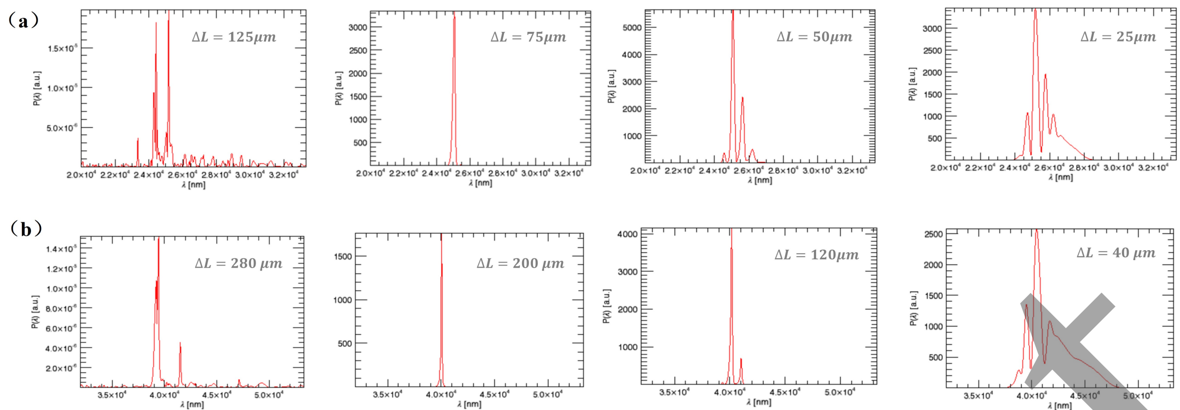

Figure 3: Saturated spectra of the mid-infrared FEL oscillator under different cavity detuning lengths: (a) operation around 25 µm and (b) operation around 40 µm.

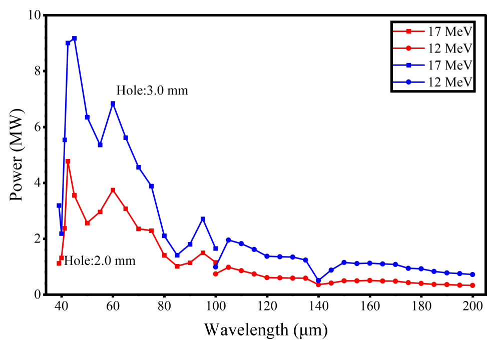

Figure 4: Calculated coupled output power in the far-infrared range for different coupling-hole sizes.

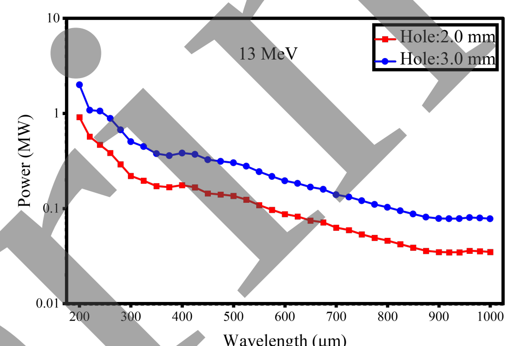

Figure 6: Calculated coupled output power in the THz range for different coupling-hole sizes.

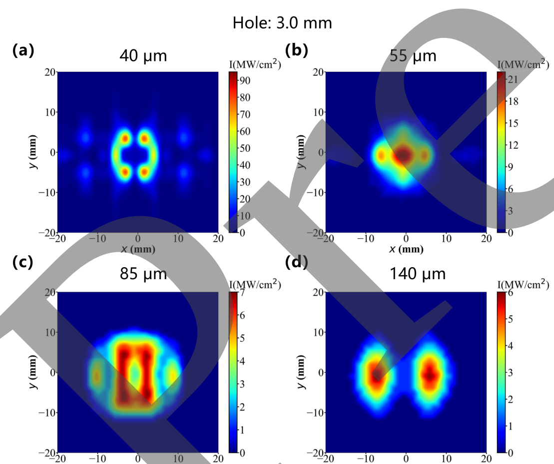

Figure 5: Transverse intensity distributions at the output mirror for representative far-infrared wavelengths. The hollow and multi-lobed patterns indicate reduced center-hole coupling efficiency.

local transverse-mode interference effect is weakened by the overall long-wavelength transmission loss, diffraction expansion and coupling-efficiency degradation. As a result, the output behavior is dominated by a smooth wavelength-dependent power decrease rather than by a distinct narrow spectral gap.

CONCLUSION

Design studies of a high-power IR-THz FEL facility based on a high-repetition-rate superconducting linac have been presented. The facility consists of an RF gun, superconducting accelerating sections, a third-harmonic linearizing cavity, a C-type bunch compressor and three oscillator beamlines covering 5 µm–1000 µm. Start-to-end simulations show that the bunch can be compressed from about 26 A to about 100 A and accelerated to about 60 MeV, while maintaining a normalized projected emittance of about 1.2 mm mrad. Based on the optimized beam parameters, oscillator simulations were performed for the mid-infrared, far-infrared and THz beamlines. The results show that cavity detuning strongly affects the mid-infrared spectrum and that waveguide-induced transverse mode evolution can lead to local reductions of the coupled output power in the far-infrared range. In the THz range, the output power decreases more smoothly with wavelength, and no pronounced narrow spectral gap is observed. These results provide a basis for further optimization of the optical cavity, coupling scheme and waveguide design.

REFERENCES

[1] J. M. J. Madey, "Free-electron lasers", *Science*, vol. 239, no. 4844, pp. 1115–1121, 1988. doi:10.1126/science.239.4844.1115

[2] G. S. Edwards *et al.*, "Free-electron-laser-based biophysical and biomedical instrumentation", *Rev. Sci. Instrum.*, vol. 74, no. 7, pp. 3207–3245, 2003. doi:10.1063/1.1584078

[3] D. D. Dlott and M. D. Fayer, "Applications of infrared free-electron lasers: basic research on the dynamics of molecular systems", *IEEE J. Quantum Electron.*, vol. 27, no. 12, pp. 2691–2703, 1991. doi:10.1109/3.104151

[4] W. Seidel, "The THz-FEL FELBE at the radiation source ELBE", in *Proc. FEL'10*, Malmö, Sweden, Aug. 2010, paper TUOCI1, pp. 209–213.

[5] G. L. Carr, M. C. Martin, W. R. McKinney, K. Jordan, G. R. Neil, and G. P. Williams, "High-power terahertz radiation from relativistic electrons", *Nature*, vol. 420, no. 6912, pp. 153–156, 2002. doi:10.1038/nature01175

[6] Y. M. Yang, G. Y. Feng, S. C. Zhang, and Z. G. He, "Longitudinal beam dynamics optimization for infrared terahertz FEL LINAC", in *Proc. LINAC'24*, Chicago, IL, USA, Aug. 2024, pp. 619–622. doi:10.18429/JACoW-LINAC2024-THPB101

[7] Y. M. Yang, G. Y. Feng, S. X. Dong, and B. X. Zhang, "Beam dynamics study for a high-repetition-rate infrared terahertz FEL facility", in *Proc. IPAC'24*, Nashville, TN, USA, May 2024, pp. 428–430. doi:10.18429/JACoW-IPAC2024-MOPG71

[8] W. Chou, "ICFA beam dynamics newsletter", no. 38, Dec. 2005. www-linac.kek.jp/mirror/icfa-bd/news.html

[9] G. Y. Feng, I. Zagorodnov, T. Limberg, *et al.*, "Beam dynamics simulation for FLASH2 HGHG option", in *Proc. LINAC'14*, Geneva, Switzerland, Aug.–Sep. 2014, paper TUPP020, pp. 471–474.

[10] G. Y. Feng, I. Zagorodnov, M. Dohlus, *et al.*, "Start-to-end simulation for FLASH2 HGHG option", in *Proc. FEL'14*, Basel, Switzerland, Aug. 2014, paper MOP083, pp. 244–247.

[11] G. Y. Feng, I. Zagorodnov, T. Limberg, *et al.*, "Beam dynamics simulations for European XFEL", DESY, Hamburg, Germany, Rep. TESLA-FEL2013-04, 2013.